Published in final edited form as:

Biosens Bioelectron. 2013 February 15; 40(1): 10–16. doi:10.1016/j.bios.2012.08.015.

Automated processing integrated with a microflow cytometer for pathogen detection in clinical matrices

J.P. Golden[1], **J. Verbarg**[1], **P.B. Howell Jr.**, **L.C. Shriver-Lake**, and **F.S. Ligler**[*]

Center for Bio/Molecular Science & Engineering, Naval Research Laboratory, Washington, DC 20375, USA

Abstract

A spinning magnetic trap (MagTrap) for automated sample processing was integrated with a microflow cytometer capable of simultaneously detecting multiple targets to provide an automated sample-to-answer diagnosis in 40 min. After target capture on fluorescently coded magnetic microspheres, the magnetic trap automatically concentrated the fluorescently coded microspheres, separated the captured target from the sample matrix, and exposed the bound target sequentially to biotinylated tracer molecules and streptavidin-labeled phycoerythrin. The concentrated microspheres were then hydrodynamically focused in a microflow cytometer capable of 4-color analysis (two wavelengths for microsphere identification, one for light scatter to discriminate single microspheres and one for phycoerythrin bound to the target). A three-fold decrease in sample preparation time and an improved detection limit, independent of target preconcentration, was demonstrated for detection of *Escherichia coli* 0157:H7 using the MagTrap as compared to manual processing. Simultaneous analysis of positive and negative controls, along with the assay reagents specific for the target, was used to obtain dose–response curves, demonstrating the potential for quantification of pathogen load in buffer and serum.

Keywords

Integrated sample processing; Microfluidics; Flow cytometry; Magnetic microspheres; Multiplexed analysis

1. Introduction

To move lab-on-a-chip (LOC) devices out of the lab and into the hands of a user usually requires integration of multiple system components. Ideally, a user would simply put a sample into a system and obtain a reliable, actionable answer (Gervais et al., 2011; Gubala et al. 2012; Ligler 2009; Yager et al., 2006). To analyze complex sample matrices (e.g. clinical fluids, environmental samples, food and beverages) with high sensitivity for targets of interest, sample processing components are necessary that are in themselves portable and automated, as well as compatible with the portable LOC analytical component. In a recent, very comprehensive review of microfluidic devices for point-of-care immunodiagnostics,

[*] Corresponding author. fligler@cbmse.nrl.navy.mil, frances.ligler@nrl.navy.mil. .

[1]Contributed equally to this manuscript.

Gervais et al. (2011) define an ideal 1$ integrated biosensor for multiplexed diagnostics that includes an input for a clinical sample, target preconcentration, microarrays of immobilized recognition molecules, sample processing reagents, mixers, valves, pumps, optics and electronics for data collection, analysis, and transmission; such a device does not yet exist, but we predict that it will (at a higher cost).

Automated sample processing using affinity reactions is generally more flexible with regard to sample type and reaction temperature, and the reagents are usually more stable than procedures employing amplification enzymes. Sample processing with affinity reagents usually involves target capture and separation from the sample matrix, followed by incubation with a series of additional binding reagents which increase the signal generated by each target to achieve the required sensitivity. Critical issues for efficiency of sample processing with affinity reagents include binding constants of recognition molecules (especially after immobilization or labeling), mixing to eliminate the formation of depletion layers at surfaces (especially with viscous samples), binding specificity of all reagents, and nonspecific binding. Most automated affinity processing systems are coupled directly to the analytical component (Gervais et al., 2011;McKenzie et al., 2009). Lateral flow immunoassays are a familiar example. However, a variety of affinity processing systems coupled with immunoassays have been reported using fluid flow driven by centrifugal force into an optically interrogated chamber (Gorkin et al., 2012; Lee et al., 2009; Peytavi et al., 2005) or by pressure-driven flow (Jokerst et al., 2010; Lafleur et al., 2012; McKenzie et al., 2009) over immobilized antibody arrays. In these reports, the higher the number of processing steps, the more complicated the device becomes. Interestingly, the degree of multiplexing does not generally have a major impact on the complexity of the processing, but is limited primarily by the cross-reactivity of the reagents used for a particular multiplexed assay.

The first step in automating sample preparation is usually target capture, preferably with target preconcentration out of larger sample volumes into μL–nL volumes, in order to take advantage of microfluidic systems that can most efficiently process small volumes. Immunomagnetic capture is a well-established technology using antibody-coated magnetic microspheres to pull target out of large volumes of sample (Palecek and Fojta, 2007). In addition to antibodies, magnetic microspheres have been coated with oligonucleotides and other capture molecules for target concentration. The advantages of using immunomagnetic microspheres for capture include stability during storage, ease of manipulation, and flexibility for use with variable sample types and volumes. The disadvantages relate more generally to use in downstream processing; in many cases, the target must be removed from the microspheres for processing and/or analysis. Kwon et al. (2008) bypassed the need to release the target from the clustered magnetic microspheres by measuring the photoinduced release of fluorescent eTags from the tracer antibodies in complexes of microspheres, capture antibody, target, and tracer antibody, but this approach requires a light-emitting diode (LED) for processing, as well as a magnet, valves and pumps, increasing the complexity of manipulations required prior to the analysis. In most of the systems reported to date, the magnetic microspheres are pulled together with a fixed magnet; this clumping can generate aggregates or sequester the target, reducing the efficiency of subsequent reagent binding or analysis. Two systems have been reported to avoid this aggregation; both use

spinning magnets that pull the microspheres continuously upstream during processing. In the processing component reported by Anderson and colleagues (Anderson et al., 2009), proteins are captured on the magnetic microspheres that are pulled upstream in a horse-shoe shaped tube, concentrated out of the sample, and then trypsinized to remove peptides from the magnetic microspheres for mass spectrometry. In the MagTrap used here, the spinning magnets pull the magnetic microspheres upstream and side-to-side during processing in a microchannel, there is no target release step, and the microspheres are released from the magnetic field for direct introduction into the analytical device (Howell et al., 2011; Verbarg et al., 2012).

Automation of sample processing and flow cytometry has been explored using large flow cytometry systems, primarily for increasing throughput. Usually, the samples are still processed (manually or robotically) in a 96-well plate and automatically sipped into a cytometer. The autonomous pathogen detection system automatically processes aqueous samples from an air collector to test for biowarfare agents using a Luminex flow cytometer and off-the-shelf fluidic components in a large free-standing system (Dzenitis and Makarewics, 2010; Hindson et al., 2005). Another interesting example of an integrated sample processing-analytical system has just been reported by Kuystermans et al. (2012) which combines the commercial FlowCytoPrep device (MSP Corp, MN) with a benchtop cytometer to monitor proliferation of cells in culture in an automated process including cell fixation and staining. Large cytometers such as the CytoBot and CytoSense have also been used to evaluate a continuous stream of algae underwater, but other than filtration through a screen, there is no sample processing involved. To our knowledge, the first report of an automated microflow cytometer was provided by James Leary's group in 2012 (Maleki et al., 2012). This whole blood analyzer labeled white cells or tumor cells with immuno-quantum dots for identification and/or immunomagnetic microspheres for sorting. The device included a micro-mixer, separation system, LED, avalanche photodiode, and electronics that operated on a 9-volt battery. Although that report focused primarily on the device rather than application data, the authors provided an elegant proof-of-principle experiment for sorting and counting CD45-positive cells.

Coded microspheres were developed in order to minimize the complexity of the optics required for multiplexed analyses (Walt, 2000). Microspheres coded with different amounts of multiple fluorophores are now widely used as substrates for multiplexed immunoassays that can be processed efficiently and analyzed using imaging or flow cytometry. We developed a microflow cytometer for analyzing multiplexed immunoassays based on a four-color analysis of fluorescently coded microspheres (Golden et al., 2010; Kim et al., 2009). Ten-plex assays in spiked buffer have demonstrated limits of detection comparable to benchtop commercial systems in assays using the same reagents, with sensitivities as low as 10 pg/ml for toxins and 10^4 cells/ml for bacteria.

In all prior reports using the microflow cytometer, sample processing was performed manually in tubes or microtiter plates. In this report, we integrate the microflow cytometer with the MagTrap sample processing component. The MagTrap does more than just trap microspheres on the side of a microfluidic channel. Spinning magnets under the channel pull the microspheres (including those with captured target) upstream against the flow and side-

to-side in the channel to both collect and concentrate the microspheres as the sample is introduced, and to expose the microspheres sequentially to the reagents (Verbarg et al., 2012). Then the rotation of the magnets is reversed, and the concentrated, but not aggregated, microspheres are released for analysis. Here we (1) improve the performance of the microflow cytometer using a streamlined fiber optic configuration, (2) connect the output from the MagTrap directly into the microflow cytometer, (3) evaluate the immunoassay results for the detection of *Escherichia coli* and (4) compare the results to the same assays performed manually. Additionally, we demonstrate that automated immunoassays can be performed in a clinical sample.

2. Material and methods

2.1. MagTrap design and function

The spinning magnetic trap, or “MagTrap”, reported in this paper combines the advantages of immunomagnetic target capture with dynamic manipulation of the magnetic microspheres inside a microfluidic channel. Permanent magnets were arranged on a rotating wheel and positioned directly beneath the microchannel, as shown in Fig. 1. The microchannel was hot embossed in polymethyl methacrylate (PMMA) from a trapezoidal mould (500 μm top width, 355 μm bottom width, 125 μm height). The magnets were placed under the narrow part of the trapezoidal channel so that trapping of the microspheres in the corners was minimized. Details of the rotating MagTrap design and function, as well as the microchannel embossing and bonding, have been previously reported (Verbarg et al. 2012).

During sample processing, the magnets rotate clockwise under the microchannel, collecting the immunomagnetic microspheres without aggregation and moving them against the flow, as well as from one side of the channel to the other. When the leading magnet rotates away from the channel, the microspheres are briefly released into the flow stream and then trapped by the next magnet. Movement of the microspheres against the flow of the incubation reagent increases the interaction of the microspheres with reagents in the flow stream. Reversal of the magnets’ rotation sweeps the microspheres downstream. When the magnets move away from the channel at the outlet, the magnetic microspheres are free to exit the device. The rotating wheel allows the microspheres to be captured, mixed, and released using permanent magnets that are always at a constant distance from the channel and need no repeated alignment. The rotational speed of the magnets was 2 rpm. This speed was optimized both for capture and movement of the beads against the 10 μl/min flow with the small, commercially available magnets used here and for the release of the beads at the same flow rate.

Although the magnetic microsphere release has been previously characterized, and limited sample processing was performed using the MagTrap, in prior experiments microsphere detection and analysis were performed separately using a commercial benchtop cytometer. This paper describes results with the integrated MagTrap and microflow cytometer device shown in Fig. 2. The integrated system was achieved by connecting the MagTrap outlet to the input of the microflow cytometer, resulting in an automated sample prep/analysis system. The integrated system features two peristaltic pumps for individual control of the core and sheath fluids. The core fluid is the sample processed through the MagTrap and into the

microflow cytometer at 10 μl/min. The sheath fluid is introduced from a single reservoir through a split tube into both sides of the core in the microflow cytometer to focus the microspheres in the interrogation region of the cytometer.

2.2. Cytometer design

The design of the grooved channel for focusing the sample stream in the microflow cytometer has been described in detail previously (Golden et al., 2009) and is shown in the lower portion of Fig. 2. Briefly, the design consists of a polydimethylsiloxane (PDMS) flow channel manufactured using soft lithography. Chevron-shaped grooves, in the top and bottom, divert the sheath fluid to fully surround the core stream containing the microspheres to be analyzed.

The organization of the fibers in the system used here is modified from previous reports for improved signal/background, especially for collecting the signal from phycoerythrin. The current microflow cytometer has four optical-fiber guide channels, for excitation and collection of fluorescence and scatter signals. Optical fibers were cleaved, placed into the guide channels and carefully aligned with the flow channel to form the interrogation region, through which the fluidic core passes. The fiber channels' heights were matched to the diameter of the fibers (130 μm) to ensure alignment of the fiber with the vertical center of the flow channel. The excitation wavelengths were provided by diode lasers at 532 nm (GM32–10 H, 10 mW, Intelite, Inc. Minden, NV) and 635 nm (LAS-200-635-15, 15 mW, Lasermax Inc., Rochester, NY), which were combined into a custom single-mode wavelength division multiplexing (WDM) fiber optic coupler (PSK-000797, Gould Technology LLC, Millersville, MD). The combined excitation light from the WDM coupler was connected to a single-mode fiber aligned to the flow channel at 90°. Fluorescence emission and scatter were collected with multimode fibers at 45° to the flow channel, and each was connected to a photomultiplier tube (PMT) (H9306-02, Hamamatsu Corp., Bridgewater, NJ) through optical filters and fiber splitters (Fiber Instrument Sales, Inc., Oriskany, NY). Large-angle scatter from the microspheres was collected at 635±5 nm. Fluorescence was collected using 665±10 nm bandpass (665DF20, Omega Optical, Inc., Brattleboro VT) and 700 nm long-pass (LL700, Corion Corp., Franklin, MA) filters for microsphere identification, and a 565±10 nm bandpass filter for detection of phycoerythrin fluorescence (565WB20, Omega Optical, Inc., Brattleboro, VT). A multimode beam-dump fiber was positioned directly across the channel from the excitation fiber to remove the majority of the excitation light, reducing the background from scattered excitation light. The output of the PMTs was recorded using an analog-to-digital converter (NI USB-6251 M, National Instruments, Austin, TX).

2.3. Cytometer software

The microspheres passing through the interrogation region generate pulses in each of the four detection channels, representing microsphere detection events. Data acquisition software, written in LabWindows/CVI (National Instruments, Austin, TX), has been updated to control pump speed and PMT gain, in addition to setting a threshold trigger value. Sample rate was set to 60 kHz. A software threshold of 0.5 V was set on the light scatter detection channel to trigger data collection of each event. When the light scatter threshold exceeded

0.5 V, the data from the two microsphere identification signals, phycoerythrin fluorescence, and light scatter were recorded until the light scatter signal dropped below the 0.5 V threshold value. Collecting data only above threshold greatly reduces the amount of data that needs to be stored.

Data analysis software was also written in LabWindows/CVI. The program loads, plots the microsphere identification data and allows the user to select clusters which correspond to the Luminex microsphere identification sets, and extracts the phycoerythrin data, mean, trimmed mean, and error statistics from the selected cluster for plotting or further analysis.

2.4. Immobilization and assays

Magnetic and polystyrene microspheres were purchased from Luminex Corp. (xMap Technology, Austin, TX, USA) and were modified with proteins using the method described by Taitt et al. (2011). Assays with polystyrene microspheres were previously reported and detected with the microflow cytometer (Golden et al., 2009; Kim et al., 2009). In order to combine the MagTrap with microflow cytometer, automated assays were performed with magnetic microspheres. The immobilized proteins included goat anti-*E. coli* O157:H7 (KPL, Gaithersburg, MD, USA) and chicken IgY on polystyrene and magnetic microspheres (Jackson Immunoresearch, Inc, West Grove, PA, USA) as a positive control along with bovine serum albumin (BSA, Sigma-Aldrich, St. Louis, MO, USA) as the negative control. Assays with the polystyrene microspheres were performed manually and included a 30-min incubation with the target. On the other hand, assays with magnetic microspheres were carried out in the MagTrap after a 20-min incubation with the target. After the target incubation, the sample was either loaded into the MagTrap or the assay proceeded manually in a Millipore MultiScreen HTS filter plate (Millipore Corp, Billerica, MA, USA). After rinsing the microspheres with PBSTB buffer (phosphate buffered saline containing 0.1% Tween 20 and 1 mg/ml bovine serum albumin (BSA), pH 7.4), they were exposed to the tracer solution (mixture of biotinylated antibodies in PBSTB) for either 30 min (filter plate) or 5 min (MagTrap) and again rinsed with the buffer. Biotinylated goat anti-*E. coli* O157:H7 (5 μg/ml) was purchased from KPL, while biotinylated rabbit anti-chicken IgY and biotinylated chicken IgY (0.75 μg/ml) was obtained from Jackson Immunoresearch. Next, the microspheres were incubated with 7.5 μg/ml streptavidin–phycoerythrin (SA-PE, Columbia BioSciences, Columbia, MD, USA) for 30 min (plate) or 3 min (MagTrap). After rinsing with buffer, the microspheres were passed through the NRL microflow cytometer for detection and analysis.

3. Results and discussion

3.1. Improved optical configuration in microflow cytometer

Microspheres were detected by the microflow cytometer optics, where each microsphere passing through the interrogation region produced a pulse recorded by the data acquisition (DAQ) software (LabWindows, National Instruments). The sets of fluorescently coded microspheres have different amounts of two fluorophores, exciting at 635 nm and emitting at 665 and 700 nm, which are used to identify them. Analysis software quantifies the signal from the pulses in each channel by calculating the area of the pulse, and plots the two

microsphere identification signals on a chart, as shown in Figs. 3 and 4a. The scatter signal was used to make sure that only single microspheres were measured and that debris and doublets were excluded. Calibrating the signal of each individual microsphere by the scatter value normalized for any variation in excitation intensity as the microsphere transited the laser beam and provided well-defined microsphere identification clusters, as reported earlier (Golden et al., 2009). The analysis software calculated the phycoerythrin signal from the microspheres in each selected cluster and reported the mean and trimmed mean (5%), standard deviation and standard error of the mean.

As shown in Fig. 2, collection fibers were aligned with the interrogation region in the flow channel at 45° with the excitation fiber. Fiber splitters were used to split the fluorescent signal from one collection fiber between the two microsphere identification PMTs and to split signal from the other collection fiber to the phycoerythrin and scatter PMTs. Since the phycoerythrin signal is very weak in comparison with the scatter signal, a 70–30 splitter was used for those wavelengths with the 70% leg carrying the phycoerythrin signal. The fiber splitters were manufactured for infrared wavelengths, and exhibited ~15% insertion loss at the wavelengths of interest, which was easily accounted for by adjusting the PMT gains. The insertion loss for the custom WDM excitation fiber coupler was measured to be 25%. Coupling, scattering and reflection losses in the flow channel resulted in the laser excitation light at the interrogation region to be 3–4 mW at each of the excitation wavelengths. Since the WDM coupler combined both excitation wavelengths into one fiber, this design only requires four optical fibers instead of six reported previously, making this design much easier to fabricate. Also, combining both excitation wavelengths into one fiber ensures that the two excitation beams are collinear, abating alignment issues inherent in the previous design. The alignment of both beams also means that the scatter signal from the 635 nm beam can now be correlated with all three fluorescent signals, if necessary. In this study, we only used scatter to normalize the bead identification (ID) fluorescence and not the phycoerythrin fluorescence, but this capability may be useful in the future.

3.2. Microsphere analysis and throughput

During sample processing, the magnetic microspheres are clearly being pulled back and forth across the channel as well as up and down. They remain separate and in motion. While the microspheres are concentrated, the magnetic field never generates clumps in any one spot. Aggregates of microspheres would be gated out of the analysis and are not included in our counts. While we eliminated the aggregation problem, we could not completely eliminate the loss of microspheres due to sticking to surfaces or trapping in tubing junctions or corners. Steps to reduce these sticking problems can include surface modification or redesign to eliminate corners (as in the use of a trapezoidal channel for the MagTrap), edges, and connectors. Different materials exhibit different degrees of surface interaction with polystyrene microspheres. Since this prototype MagTrap-microflow cytometer included components made out of polyetheretherkeytone (PEEK; tubing), polymethylmethacrylate (PMMA; MagTrap) and polydimethylsiloxane (PDMS; cytometer), the microsphere throughput of the system was of concern and recovery experiments were designed to evaluate throughput of the microspheres in the combined system.

In these experiments, microspheres were continuously introduced at ~50 microspheres/ μL at a flow rate of 10 μL/min either into the flow cytometer alone or into the MagTrap attached directly to the microflow cytometer. The microspheres were then counted for 5-min intervals using the microflow cytometer. The experiment demonstrated that the microspheres could be analyzed in a straight-through, multi-component system, but that about 30% of the microspheres were lost from the analysis. Without the MagTrap, the microsphere counts were 650±150 microspheres/min while with the MagTrap, the counts were 440±160 microspheres/min. Careful inspection indicated that microspheres did accumulate over time at the junctions between the components; such junctions will be eliminated as the two devices are integrated in a single substrate. Coating surfaces with films such as polyethylene oxide is another possibility, but there did not seem to be a general buildup of microspheres adhering to any of the surfaces. Since all the beads were exposed to the reagents, the reduced concentration of beads introduced into the microflow cytometer did not impact the assay data and statistics, as long as comparable numbers of beads were analyzed. The only impact was that the time required to count the same number of beads was slightly longer.

As can be seen in Figs. 3 and 4a, the clusters created by the individual microsphere sets have a characteristic diagonal spread. The spread is more pronounced in the raw data, as the fluorescent signal is proportional to the illumination intensity, and that intensity changes as a result of the varying positions of the microspheres in the fluid core. Fortunately, the light scatter signal is also proportional to the illumination intensity, so normalizing the two microsphere identification channels to light scatter removes much of the diagonal variation. There is still some variation, however, and the variation within a single bead set appears to be more pronounced for the magnetic microspheres than for the nonmagnetic microspheres. One possibility is that slight differences in the amount of iron in each of the microspheres causes variation in the light scatter signal from individual magnetic microspheres, reducing the effectiveness of using light scatter for normalizing the two fluorescent signals used for the identification. Fortunately, the availability of a wide range of microsphere sets allows for strategic selection of sets to accommodate the degree of spread seen here without overlap.

3.3. Immunoassay using the integrated system

Using a mixture of three appropriately modified microsphere sets, positive (Chicken IgY) and negative (BSA) control assays were run simultaneously with the *E. coli* samples. Microspheres were incubated with the capture antibodies for 20 min (magnetic microspheres) or the standard 30 min (nonmagnetic microspheres). While we did reduce the incubation time slightly for the initial capture step using magnetic microspheres, we did not try to minimize the capture time because future users will have to optimize it for their individual targets, antibody affinities, sample viscosities, and sample volumes. The normalized signals were calculated for the *E. coli* set by first subtracting the mean negative control signal from the mean signal of the *E. coli* set and then dividing by the mean positive control signal. The BSA controlled for the effects of baseline drift and the chicken controlled for the effects of run-to-run variations. The values for each microsphere in the set were then averaged to obtain the mean for the particular *E. coli* concentration.

In order to compare the MagTrap to manual processing, both polystyrene and magnetic microspheres were used. Based on the microsphere fluorescence and scatter, the clusters for the magnetic microsphere identification plots (Fig. 4a) appear more spread out than those of the polystyrene microspheres used in the manual assay (Fig. 3a), which means fewer simultaneous assays can be performed on the magnetic microspheres. The magnetic microspheres contain iron and are larger in size (~7 μm vs ~5 μm in diameter). We cannot rule out that the magnetic microspheres are slightly more heterogeneous in size, with a correspondingly increased variability in fluorescence, but the presence of the iron is probably sufficient to increase the variability in the scatter signals used for normalization. Nonetheless, the microsphere sets selected had sufficiently distinct fluorescence profiles that they could be easily distinguished for these experiments.

Three sets of MagPlex microspheres were prepared for the detection of *E. coli*, binding of chicken IgY (positive control), and assessment of nonspecific binding (BSA-coated, negative control microspheres). The MagTrap was used to process buffer and 10% human serum samples spiked with 1×10^3, 1×10^4, 1×10^5, and 1×10^7 cells/ml *E. coli* directly through the microflow cytometer. The resulting dose–response curves are shown in Fig. 4b. Results show that *E. coli* could be detected at concentrations above ~1×10^4 cells/ml in both the buffer and 10% serum with the MagTrap, which is comparable to manual assays performed on the polystyrene microspheres (Fig. 3b).

With the MagTrap automated processing system, the detection limit was lowered from 10^5 cells/mL to 10^4 cells/mL in buffer or serum. This suggests that the dynamic mixing within the MagTrap improved both the binding of tracer antibodies to captured antigen and the SA-PE binding to the biotinylated tracers. In the manual assays, the polystyrene microspheres, if not continually shaken during the incubations, will settle, which can limit the availability of binding sites due to steric hindrance. Furthermore, particles of this size and density do not have sufficient Brownian motion to disrupt the formation of depletion layers at their surfaces when active mixing is not provided (Jennings et al., 2008).

In situations of inefficient mixing during the incubation, depletion layers can form at the surface of the microspheres where the reagent concentration is diffusion limited. In our assays, the manually processed microspheres were continually shaken during the incubation, so those factors are not likely to have played a major role in the difference seen here. However, collecting the microspheres between each step either through a filter plate or using a magnet to collect the magnetic microspheres to the side may have produced aggregates during the processing which were not completely exposed to reagent prior to pipetting and introduction into the microflow cytometer. Another explanation is that the microspheres are simply not moving through the reagents as fast. Based on the specified size and density of the magnetic microspheres, they have a mean settling velocity on the order of 2.3 μm/s; shaking would only marginally increase this velocity. In the MagTrap, by contrast, the mean flow velocity is 3100 μm/s. When being dragged, the microspheres are travelling at speeds of up to 750 μm/s against the flow. As a result, a microsphere will sample a much larger volume of solution in the MagTrap in a given period of time.

Either due to the dynamic exposure to the reagents or to the elimination of the less reproducible manual manipulations, the coefficient of variation (CV) in the data was less for the samples processed through the MagTrap than the manual method. The manually processed samples had CVs of 89% and 79% for buffer and serum, while the automatically processed samples had corresponding CVs of 45% and 21%. Manual processing consists of discrete pipetting steps, during which errors can be introduced. On the other hand, the automated processing is done at constant flow rates and in set time periods, thus making the process more reproducible.

For the analysis of clinical and environmental samples, it is useful to handle samples with different viscosities. Only the first trapping step would be impacted by a high viscosity sample because the sample matrix is removed prior to any reagent addition. During this period, if the sample is of significantly higher viscosity than those used here, the magnetic force, rotation speed, and flow rate would have to be rebalanced to optimize trapping in the particular matrix of interest or the matrix diluted prior introduction into the MagTrap (as done here). This tradeoff can be modeled since the magnetic field, flow rate, rotation rate, and viscosity are known quantities—making the adaptation to particular applications relatively straightforward.

Perhaps of more significance is that the improvement in results was achieved while the processing time decreased from 100 min to 38 min. It may be possible to further shorten the reagent incubation and wash times or even eliminate the final wash. We have not yet tried to decrease the time for the tracer incubation step, because it may be dependent on antibody avidity or sample viscosity, and thus the initial time for target capture should be optimized for the lowest affinity antibody in a specific multiplexed assay. Depending on the avidity of the capture antibodies and the volume of sample, the initial capture step could also be performed in the MagTrap. Decreasing or eliminating the wash steps could easily subtract another 8–10 min from the total manual assay time.

4. Conclusion

A microfluidic sample processing component was integrated with a microflow cytometer to provide a proof-of-principle demonstration. The MagTrap sample processing device can concentrate magnetic microspheres with captured target out of an arbitrary volume of sample and process it with multiple reagents prior to release into a microflow cytometer for analysis. Magnets within a spinning wheel below a trapezoidal channel move the microspheres upstream and side-to-side to mix them with reagent very efficiently. Simply reversing the direction of rotation of the magnets sweeps the microspheres into the flow cytometer for analysis. There is no need to move the magnets away from the channel, which should facilitate manufacturing by eliminating the need for repetitive realignment of the magnets. Even with a reduction in the assay time from 100 min to 38 min, the limit of detection was improved by an order of magnitude. The automated processing can eliminate manual manipulations; the operator no longer has to pipette reagents or transfer processed microspheres to the cytometer. As in other automated systems, the data from this proof-of-principle immunoassay demonstrates the corresponding decrease in the coefficient of variation in the data. With further refinements, the integrated system described here would

be an excellent fit for point-of-care diagnostics, periodic monitoring of environmental samples (air or water), and clinical analysis in resource-limited environments with a shortage of trained personnel.

Acknowledgments

The work presented here was performed under NIH Grant U01 A1075489 and ONR/NRL 6.2 work unit 6336. J.V. is a National Research Council postdoctoral fellow. The views presented are those of the authors and do not represent the opinion or policy of the National Institutes of Health, Department of Health and Human Service, the US Navy, or the Department of Defense.

References

Anderson NL, Jackson A, Smith D, Hardie D, Borchers C, Pearson TW. Molecular & Cellular Proteomics. 2009; 8(5):995–1005. [PubMed: 19196707]

Dzenitis, JM.; Makarewicz, AJ. The Microflow Cytometer. Kim, JS.; Ligler, F., editors. Pan Stanford Publishing Pte Ltd; Singapore: 2010. p. 263-286.

Gervais L, de Rooij N, Delamarche E. Advanced Materials. 2011; 23(24):H151–H176. [PubMed: 21567479]

Golden JP, Kim J, Anderson GP, Hashemi N, Howell PJ, Ligler FS. A Microflow Cytometer on a Chip. SPIE. 2010; 7553:755308-1–755808-6.

Golden JP, Kim JS, Erickson JS, Hilliard LR, Howell PB, Anderson GP, Nasir M, Ligler FS. Lab on a Chip. 2009; 9(13):1942–1950. [PubMed: 19532970]

Gorkin R, Park J, Siegrist J, Amasia M, Lee BS, Park J-M, Kim J, Kim H, Madou M, Cho Y-K. Lab on a Chip. 2012; 10(14):1758–1773. [PubMed: 20512178]

Gubala V, Harris LF, Ricco AJ, Tan MX, Williams DE. Analytical Chemistry. 2012; 84:487–515. [PubMed: 22221172]

Hindson BJ, Makarewicz AJ, Setlur US, Henderer BD, McBride MT, Dzenitis JM. Biosensors & Bioelectronics. 2005; 20(10):1925–1931. [PubMed: 15741059]

Howell PB Jr. Eitel R, Golden J, Ligler FS. Rotationally Actuated Magnetic Bead Trap and Mixer. Aug 4.2011 2011. US20110188339 and WO2011094555.

Jennings TL, Rahman KS, Fournier-Bidoz S, Chan WCW. Analytical Chemistry. 2008; 80(8):2849–2856. [PubMed: 18307362]

Jokerst JV, Jacobson JW, Bhagwandin BD, Floriano PN, Christodoulides N, McDevitt JT. Analytical Chemistry. 2010; 82(5):1571–1579. [PubMed: 20128622]

Kim JS, Anderson GP, Erickson JS, Golden JP, Nasir M, Ligler FS. Analytical Chemistry. 2009; 81(13):5426–5432. [PubMed: 19496600]

Kuystermans D, Mohd A, Al-Rubeai M. Methods. 2012; 56:358–365. [PubMed: 22445707]

Kwon Y, Hara CA, Knize MG, Hwang MH, Venkateswaran KS, Wheeler EK, Bell PM, Renzi RF, Fruetel JA, Bailey CG. Analytical Chemistry. 2008; 80(22):8416–8423. [PubMed: 18847280]

Lafleur L, Stevens D, McKenzie K, Ramachandran S, Spicar-Mihalic P, Singhal M, Arjyal A, Osborn J, Kauffman P, Yager P, Lutz B. Lab on a Chip. 2012; 12(6):1119–1127. [PubMed: 22311085]

Lee BS, Lee J-N, Park J-M, Lee J-G, Kim S, Cho Y-K, Ko C. Lab on a Chip. 2009; 9(11):1548–1555. [PubMed: 19458861]

Ligler FS. Analytical Chemistry. 2009; 81(2):519–526. [PubMed: 19140774]

Maleki T, Fricke T, Quesenberry JT, Todd PW, Leary JF. Point-of-care, portable microfluidic blood analyzer system. Proc. SPIE. 2012; 8251:82510C-1–82510C1-3.

McKenzie KG, Lafleur LK, Lutz BR, Yager P. Lab on a Chip. 2009; 9(24):3543–3548. [PubMed: 20024034]

Palecek E, Fojta M. Talanta. 2007; 74(3):276–290. [PubMed: 18371642]

Peytavi R, Raymond FR, Gagne D, Picard FJ, Jia G, Zoval J, Madou M, Boissinot K, Boissinot M, Bissonnette L, Ouellette M, Bergeron MG. Clinical Chemistry. 2005; 51(10):1836–1844. [PubMed: 16109708]

Taitt, CR.; Shriver-Lake, LC.; Anderson, GP.; Ligler, FS. Biomedical Nanotechnology. Hurst, SJJ., editor. Humana Press; 2011. p. 77-94.

Verbarg J, Kamgar-Parsi K, Shields AR, Howell PB, Ligler FS. Lab on a Chip. 2012; 12:1793–1799. [PubMed: 22344487]

Walt DR. Science. 2000; 287(5452):451–452. [PubMed: 10671175]

Yager P, Edwards T, Fu E, Helton K, Nelson K, Tam MR, Weigl BH. Nature. 2006; 442(7101):412–418. [PubMed: 16871209]

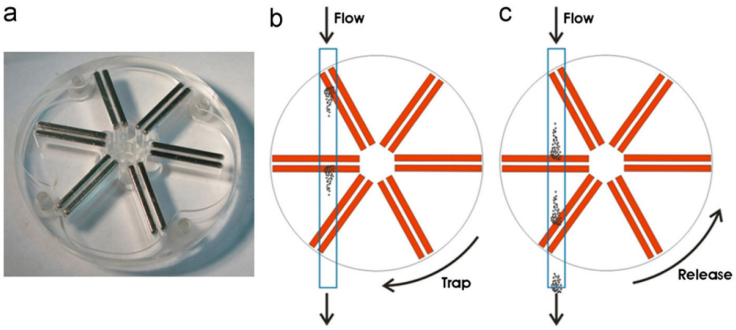

Fig. 1.

Spinning magnetic trap concentrates immunomagnetic microspheres from a sample stream and moves them continually. (a) Photo of MagTrap wheel showing strip magnets. (b) Pulling the microspheres upstream against the flow while simultaneously moving them from one side of the channel to the other concentrates the microspheres and enhances interaction with reagents (trap). (c) When exposure to the reagents is complete, the rotation of the magnets is reversed, and the microspheres are released downstream into an interrogation device (release).

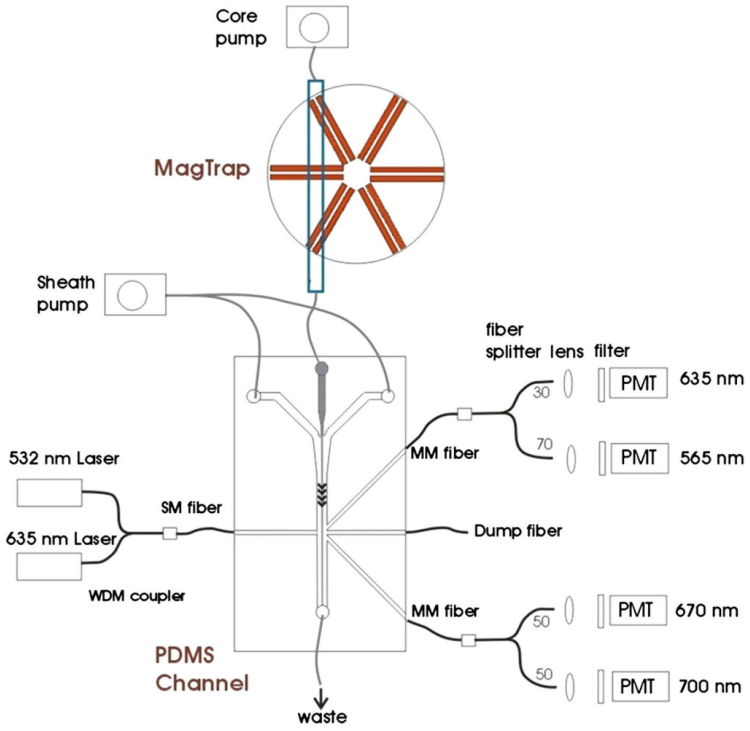

Fig. 2.

System overview diagram depicting the fluidic and optical connections for the MagTrap-microflow cytometer assembly.

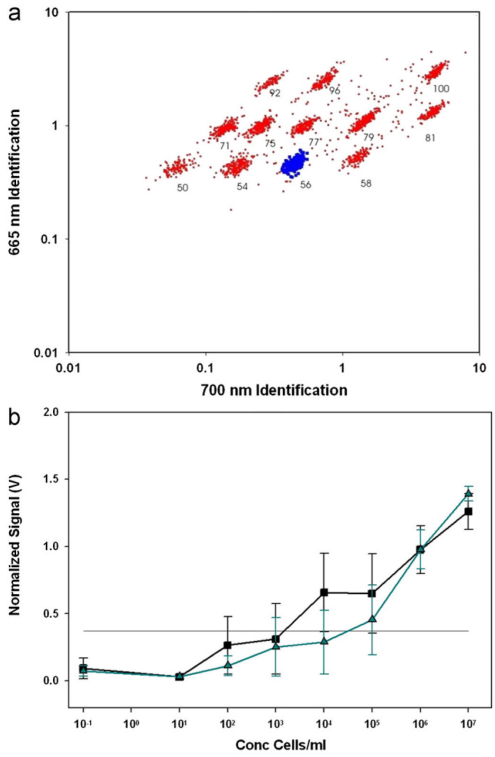

Fig. 3.

ID plot for nonmagnetic microspheres (a) and dose–response for *E. coli* (b) in PBSTB buffer (square) and 10% serum (triangle). Cluster 56 microspheres were specific for the *E. coli* assay. Assays for chicken and BSA on microsphere sets 54 and 75, respectively, were positive and negative controls. The *E. coli* signal shown in (b) was normalized to the chicken signal, above the BSA threshold. Error bars are SEM. Threshold value was calculated to be 3 standard deviations above the blank signal (gray line).

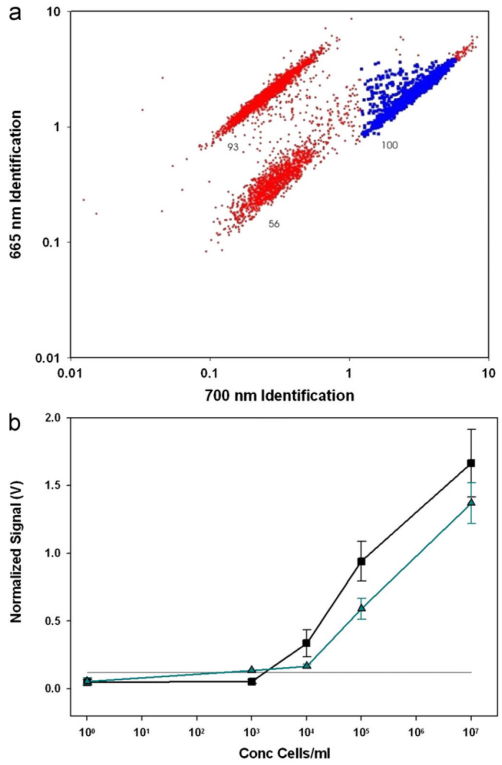

Fig. 4.

ID plot for magnetic microspheres (a) and dose–response curve for *E. coli* (b) in PBSTB buffer (square) and 10% serum (triangle) using the MagTrap and three sets of magnetic Luminex microspheres for automated sample preparation. Cluster 100 microspheres were prepared for the detection of E coli, while cluster 93 was for detection of chicken (positive control). Cluster 56 microspheres were coated with BSA and served as the negative control. *E. coli* response was normalized to the chicken signal, above the BSA threshold. Error bars are SEM. Threshold value was calculated to be 3 standard deviations above the blank signal (gray line).